MOAO Real-Time LQG implementation on CANARY

G. SIVO[1,2a], C. KULCSÁR[1], H.-F. RAYNAUD[1], J.-M CONAN[2], É. GENDRON[3], and F. VIDAL[3]

[1] Laboratoire de Traitement et de Transport de l'Information, Institut Galilée, Université Paris 13, Villetaneuse, France
[2] Onera - the French Aerospace Lab, F-92322 Châtillon, France
[3] Laboratoire d'Études Spatiales et d'Instrumentation en Astrophysique, Observatoire de Paris, Meudon, France

Abstract. Single Conjugated Adaptive Optics is a proven technique used in order to correct the effect of atmospheric turbulence and telescope vibrations. The corrected field of view (FoV) is however limited by the anisoplanatism effect. Many concepts of Wide Field AO (WFAO) systems are under study, especially for the design of Extremely Large Telescopes (ELTs) instruments. Multi-Object Adaptive Optics (MOAO) is one of these WFAO concepts that is particularly suited for high redshifts galaxies observations in very wide FoV. The E-ELT instrument EAGLE will use this approach. CANARY, the on-sky pathfinder for MOAO, obtained the first compensated images on Natural Guide Stars (NGSs) at the William Herschel Telescope in September 2010. The control and performance optimization of such complex system are a key issue. Linear Quadratic Gaussian (LQG) control is an appealing strategy that provides optimal control for an explicit minimum variance performance criterion. It also provides a unified formalism that allows accounting for specific multi WF Sensing (WFS) channels, both for Laser Guide Stars (LGSs) and NGSs, and for various disturbance sources (turbulence, vibrations). Furthermore, preliminary simulation results suggest that performance can be significantly improved with tomographic LQG control compared to MMSE static reconstruction. Our objective is to obtain a first on-sky demonstration of tomographic LQG control during CANARY Phase B, featuring LGS and NGS WFSs. We show how the specific MOAO CANARY configuration can be embedded in a state-space framework and we present how this control law can be implemented onto the Real-Time Computer (RTC). The state-space model includes: stochastic autoregressive models of order 2 for the turbulent phase in each layer and for vibrations affecting the telescope; LGS and NGS measurement equations; DM model and delays in the loop. Model identification and off-line calculations necessary for a robust on-sky operation are discussed.

1 Introduction

Adaptive Optics (AO) [15] is a technique that compensates in real-time the wavefront (WF) of the light coming from a so-called guide star. The WF is distorted after propagation through the atmosphere. The success of AO is such that the next generation of telescopes, as the European Extremely Large Telescope (E-ELT), cannot be conceived without it. Many concepts of new AO systems working on a wide field of view (WFAO) are required in order to carry out the future astrophysical programs such as ground layer AO (GLAO) [11] or multi-conjugate AO (MCAO) [8]. The so-called multi-object AO (MOAO) technique was introduced for the first time by [7], for analysing the morphology of high-redshifts galaxies. The E-ELT instrument EAGLE [5] will use this technique. CANARY [12] is the on-sky pathfinder for MOAO. It obtained the first compensated images on Natural Guide Stars (NGSs) at the 4.2 m *William Herschel Telescope*, Canary Islands, in September 2010 [6]. In this paper we present our strategy for the on-sky validation of optimal control in MOAO. Firstly (Sect. 2), we present the dynamical model used for describing the disturbance of the WF and the performance obtained with the CANARY pathfinder using a Linear Quadratic Gaussian (LQG) control. Secondly (Sect. 3) we present the implementation of this control law on the CANARY system.

[a] gaetano.sivo@univ-paris13.fr

2 Model building and LQG performance

2.1 Model building

In order to solve the optimal control problem, it is necessary to model the evolution of the perturbation phase in time, both for turbulence φ_k^{tur} and vibrations ϕ_k^{vib}. Throughout this paper, we will distinguish the phase in the volume denoted by φ and the resulting phase in a direction of interest denoted by ϕ. For the turbulence we can therefore write:

$$\phi_k^{\text{tur}} \triangleq M^{\text{obj}} \varphi_k^{\text{tur}} \tag{1}$$

where M^{obj} is the operator that extracts and sums the phase's footprints in the direction of the object of interest. A widely used class of models to describe the phase's distortion is the class of vector-valued autoregressive (AR) processes. The phases are here decomposed on a Zernike basis [17]. In the context of CANARY, first studies (see Sect. 2.2) show that an AR model of order 2 (AR2) for the turbulent phase on each layer leads to good performance. The turbulent phase, evolving in layer ℓ can therefore be written as:

$$\varphi_{k+1}^{\text{tur},\ell} = A_1^{\text{tur},\ell} \varphi_k^{\text{tur},\ell} + A_2^{\text{tur},\ell} \varphi_{k-1}^{\text{tur},\ell} + v_k^{\text{tur},\ell} \tag{2}$$

where $v_k^{\text{tur},\ell}$ is a Gaussian white noise with covariance matrix $\Sigma_v^{\text{tur},\ell}$. Turbulence layers are assumed to be independent from each others, so that the turbulent phase in the volume is just the concatenation of the phase in each layer, leading to

$$\varphi_{k+1}^{\text{tur}} = A_1^{\text{tur}} \varphi_k^{\text{tur}} + A_2^{\text{tur}} \varphi_{k-1}^{\text{tur}} + v_k^{\text{tur}} \tag{3}$$

where A_1^{tur} and A_2^{tur} are bloc diagonal matrices formed with $A_1^{\text{tur},\ell}$ and $A_2^{\text{tur},\ell}$ respectively. The vibrations affecting the system can also be modelled by an AR2 [10]. For a given vibration i, we obtain:

$$\phi_{k+1}^{\text{vib,i}} = A_1^{\text{vib,i}} \phi_k^{\text{vib,i}} + A_2^{\text{vib,i}} \phi_{k-1}^{\text{vib,i}} + v_k^{\text{vib,i}} \tag{4}$$

The global resulting phase can be written as:

$$\phi_k = \phi_k^{\text{tur}} + \phi_k^{\text{vib}} = \phi_k^{\text{tur}} + \sum_{i=1}^{n_v} \phi_k^{\text{vib,i}} \tag{5}$$

Vibrations affect in practice mainly the tip/tilt components of the phase. The CANARY bench will use during phase B Laser Guide Stars (LGSs) and Natural Guide Stars (NGSs) for tomographic reconstruction, leading to measurement equations:

$$y_k^{\text{ngs,i}} = D^{\text{ngs,i}} (M^{\text{ngs,i}} \varphi_{k-1}^{\text{tur}} + \phi_{k-1}^{\text{vib}}) + w_k^{\text{ngs,i}} \tag{6}$$

$$y_k^{\text{lgs,i}} = D^{\text{lgs,i}} M^{\text{lgs,i}} \varphi_{k-1}^{\text{tur}} + w_k^{\text{lgs,i}} \tag{7}$$

The matrix $M^{\text{ngs,i}}$ resp. $M^{\text{lgs,i}}$ extracts and sums the phase's footprints in the directions of measurement corresponding to the NGS's resp. LGS's angular positions (cylindrical resp. conical projectors), and D^{ngs} resp. D^{lgs} is the WF sensor (WFS) matrices for natural resp. laser guide stars. Measurement noises $\{w^{\text{ngs}}\}$ and $\{w^{\text{lgs}}\}$ are supposed to be white Gaussian noises independent of $\{v^{\text{tur}}\}$ and $\{v^{\text{vib}}\}$, with covariance matrices $\Sigma_{w^{\text{ngs}}}$ and $\Sigma_{w^{\text{lgs}}}$ respectively. As mean slopes are removed from LGS measurements, vibrations do not affect y^{lgs}. Mean slopes removal is here incorporated in D^{lgs}. If we denote by $\underline{D}^{\text{lgs}}$ the WFS matrix without mean slopes removal and by $\underline{y}_k^{\text{lgs}}$ and $\underline{w}_k^{\text{lgs}}$ the corresponding measurement equation and noise at the time step k, we have

$$\underline{y}_k^{\text{lgs,i}} = \underline{D}^{\text{lgs,i}} M^{\text{ngs,i}} \varphi_{k-1}^{\text{tur}} + \underline{w}_k^{\text{lgs,i}} \tag{8}$$

Hence, $y_k^{\text{lgs,i}}$ is linked to $\underline{y}_k^{\text{lgs,i}}$ through:

$$y_k^{\text{lgs,i}} = \begin{pmatrix} I - \frac{1}{n_s}\mathbf{1} & 0 \\ 0 & I - \frac{1}{n_s}\mathbf{1} \end{pmatrix} \underline{y}_k^{\text{lgs,i}} \triangleq P_{\text{rem}}^{\text{lgs,i}} \underline{y}_k^{\text{lgs,i}} \tag{9}$$

where $\mathbf{1}$ is a squared matrix full of 1. Consequently, if $\underline{w}_k^{\text{lgs,i}}$ denotes the measurement noise before mean slopes removal, its variance is related $\Sigma_w^{\text{lgs,i}}$ through:

$$\Sigma_w^{\text{lgs,i}} \triangleq \text{Var}(w_k^{\text{lgs,i}}) = P_{\text{rem}}^{\text{lgs,i}} \text{Var}(\underline{w}_k^{\text{lgs,i}}) P_{\text{rem}}^{\text{lgs,i}^T} \tag{10}$$

Simple rearrangements show that all the models presented above can be written in standard state-space form as:

$$\begin{cases} x_{k+1} = Ax_k + \Gamma v_k \\ y_k = Cx_k + w_k \\ \phi_k = C_\phi x_k \end{cases} \tag{11}$$

The disturbance in the direction of interest ϕ_k is obtained as an output of the state model. The state vector in this case can be simply chosen as the concatenation of turbulence and vibration phases:

$$x_k \triangleq \begin{pmatrix} x_k^{\text{tur}} \\ x_k^{\text{vib}} \end{pmatrix}, \quad x_k^{\text{tur}} \triangleq \begin{pmatrix} \varphi_k^{\text{tur}} \\ \varphi_{k-1}^{\text{tur}} \end{pmatrix}, \quad x_k^{\text{vib}} \triangleq \begin{pmatrix} x_k^{\text{vib},1} \\ x_k^{\text{vib},2} \\ \vdots \\ x_k^{\text{vib},n_v} \end{pmatrix}, \quad x_k^{\text{vib,i}} \triangleq \begin{pmatrix} \phi_k^{\text{vib,i}} \\ \phi_{k-1}^{\text{vib,i}} \end{pmatrix} \tag{12}$$

All the matrices present in this system can be deduced from Eq. (2) to (12).

The control objective is to minimize the averaged residual phase variance $\phi_k^{\text{res}} \triangleq \phi_k - \phi_k^{\text{cor}}$ where $\phi_k^{\text{cor}} = Nu_{k-1}$, u_{k-1} is the control vector at time $k-1$ and N is the influence matrix. The influence matrix N is the operator that connects voltages u to Zernike modes as shown in [14] for an MCAO configuration. This leads to the following performance criterion:

$$J(u) = \lim_{K \to +\infty} \frac{1}{K} \sum_{k=1}^{K} \|\phi_{k+1} - Nu_k\|^2 \tag{13}$$

which optimal solution is known to be given by the Linear Quadratic Gaussian (LQG) control:

$$u_k^* = P_u \widehat{\phi}_{k+1|k} \tag{14}$$

where

$$\widehat{\phi}_{k+1|k} \triangleq \text{E}[\phi_{k+1} | y_k, \ldots, y_0] \tag{15}$$

is the conditional expectation of ϕ_{k+1} knowing all the measurements $y_k, \ldots, y_0$ and P_u is the projector defined as the Moore-Penrose pseudo-inverse of N [13]. In other words, the optimal control corresponds to project onto the DM space the optimal prediction $\widehat{\phi}_{k+1|k}$, which is computed recursively as the output of the Kalman filter based on Eq. (11). We remind that CANARY is an open loop control bench, apart from a steering mirror for the LGS stabilization working in closed loop.

Since we have expressed our control solution, based on explicit dynamical models, we are now able to estimate the performance on CANARY.

2.2 LQG MOAO performance

We present in this section the performance results using a LQG control law on the CANARY system. Different hypothesis are tested for these simulations. The parameters used for these simulations are the

following. We have a 4.2m telescope, 3 layers of turbulence with a corresponding relative C_n^2 profile given by $[0.5, 0.17, 0.33]$. The layers are located at $[0, 2000, 4000]$ meters with respective wind speeds of $[7.5, 12.5, 15]$ m/s. We have deliberately excluded the high altitude layers that are not seen by the Rayleigh LGS. The turbulence is simulated according to the Von Kármán law and the translation of the phase screens are done using the frozen flow hypothesis. We assume also that we do not have vibrations affecting the system. The guide stars are a square constellation of radius 30 arcsec. They represent the LGS configuration but we do not account for Tip Tilt indetermination and cone effect specificities. We use a single DM conjugated to the pupil that provides the on-axis correction.

Concerning the LQG dynamical models, they are constructed assuming a well calibrated system, meaning that we know the values of the guide star angular positions, the seeing and turbulence profile, the DM influence matrix [16]. We recall that the temporal prior is a modal AR2 model that is based on assumptions on the wind profile, in modulus. We test hereafter the robustness in performance with respect to wind speed uncertainties.

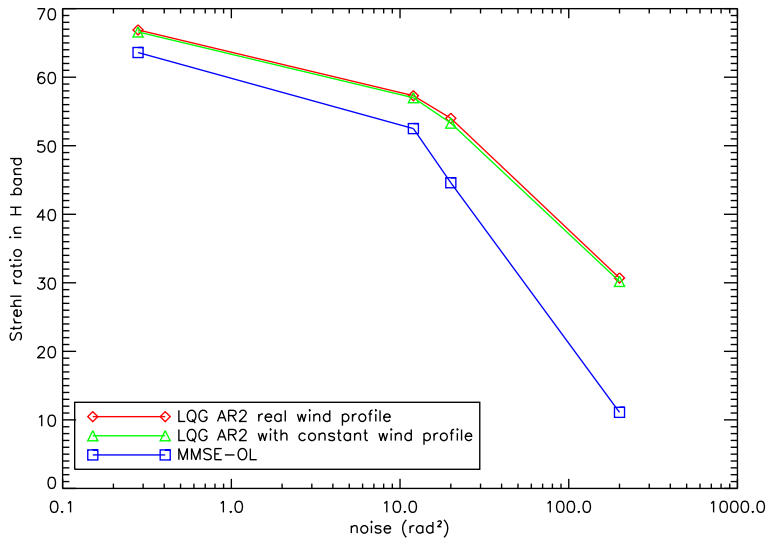

Fig. 1. On-axis Strehl ratio in H band ($1.65\mu m$), obtained for different control laws, as a function of the wavefront sensing noise level.

We see in Fig. 1 that the LQG performance is higher than with a classical control based on static minimum mean square error (MMSE) reconstruction. We see also that LQG control is more robust to high WFS noise level. At the nominal CANARY LGS measurement noise variance, that is 0.28 rad^2, Strehl ratio is 5% higher in H-band. The gain is even more important when the measurement noise level increases.

Since it is very difficult to have a good knowledge on the wind speed profile, we have studied the impact of wind profile uncertainties. In this robustness study, we always keep the same true profile to generate turbulence while exploring various wind priors used in the LQG control. The performance obtained with wind speeds in all layers set to the average wind speed value, that is 11.2 m/s, is displayed in Fig. 1. Performance is hardly affected. We have also performed simulations with more drastic uncertainties on the wind speed values: factor 10 weaker, or stronger, than mean wind speed, and also values 40% larger, or smaller, than the true wind profile. The results are summarized in the table 1.

We clearly see that an overestimation of the wind speed is more penalizing that an underestimation. Besides, 40% errors lead to only a few percent of loss in performance. Of course eventually performance collapses with a severe, and non realistic, overestimation of the speed, set here to 112 m/s.

Table 1. Performance obtained using a LQG controller with different wind speed profile priors (indicated in the table in m/s) for the control model. The true wind profile used to generate the turbulence is in all cases [7.5, 12.5, 15] m/s.

Control with:	Wind speed value on layer 1	on layer 2	on layer 3	Strehl ratio in H-band
True profile	7.5	12.5	15	0.68
Mean speed	11.2	11.2	11.2	0.68
Mean speed ÷ 10	1.12	1.12	1.12	0.66
Mean speed × 10	112	112	112	0.09
True profile − 40%	4.5	7	9	0.70
True profile + 40%	10.5	17	21	0.66

In conclusion LQG control, thanks to spatial and temporal priors, improves MOAO performance, compared to a static MMSE control. Gains are even higher in low WFS signal to noise ratio conditions. Besides, LQG exhibits a good robustness to wind speed profile uncertainties. Wind speed could for instance be set in all layers to an approximate mean value obtained by standard data reduction applied on WFS time series. These results are quite promising for on-sky operation.

3 LQG control implementation in CANARY

Real-time implementation of the Kalman filter reduces to the so-called update and prediction equations:

$$\begin{cases} \widehat{x}_{k|k} = \widehat{x}_{k|k-1} + H_\infty(y_k - C\widehat{x}_{k|k-1}) \\ \widehat{x}_{k+1|k} = A\widehat{x}_{k|k} \end{cases} \tag{16}$$

The Kalman gain is computed off-line as:

$$H_\infty \triangleq \Sigma_\infty C^T (C\Sigma_\infty C^T + \Sigma_w)^{-1} \tag{17}$$

where Σ_∞ is the solution of the discrete Algebraic Riccati equation:

$$\Sigma_\infty = A\Sigma_\infty A^T + \Gamma\Sigma_v\Gamma^T - A\Sigma_\infty C^T (C\Sigma_\infty C^T + \Sigma_w)^{-1} C\Sigma_\infty A^T \tag{18}$$

Equation (16) can be replaced by the single recursive equation.

$$\widehat{x}_{k+1|k} = (A - L_\infty C)\widehat{x}_{k|k-1} + L_\infty y_k \tag{19}$$

where $L_\infty \triangleq AH_\infty$.

The CANARY Real-Time Computer (RTC) developed by the University of Durham (see [1]) and, a generic observer structure, is implemented [14] under the form:

$$\begin{cases} z_{k+1} = M_1 z_k + M_2 y_k + M_2 M_3 u_{k-2} \\ u_k = M_4 z_{k+1} \end{cases} \tag{20}$$

where z_k is the controller state. The Kalman filter (19) is obtained with:

$$\begin{cases} M_2 = L_\infty \\ M_1 = A - M_2 C \\ M_3 = \begin{cases} DN \text{ if closed loop} \\ 0 \text{ if open loop} \end{cases} \\ M_4 = P_u C_\phi \end{cases} \tag{21}$$

So that $z_{k+1} = \widehat{x}_{k+1|k}$.

For CANARY, the typical size of x, y and u are respectively $2(410 + 20) = 860$, $8 \times 72 = 576$ and $52 + 4 = 56$, from which one can deduce the matrix sizes. The advantage of the general formulation given above, with full size matrix vector multiply, is the flexibility. Of course when moving to more complex systems for VLTs, or even ELTs, both off-line and on-line calculations may become an issue. However various approaches have been recently proposed to overcome this problem by taking advantage of the particular structure of the operations (linear shift invariance, sparsity...) [4], [9].

4 Conclusion and perspectives

We have shown how the specific MOAO CANARY configuration can be embedded in a state-space framework and have presented how this control law can be implemented onto the RTC. The state-space model includes: stochastic autoregressive models of order 2 for the turbulent phase in each layer and for vibrations affecting the telescope; LGS and NGS measurement equations; DM model and delays in the loop.

We have demonstrated through numerical simulations the gain in performance brought by LQG control compared to more a standard static MMSE approach. Improvements are higher in low WFS signal to noise ratio conditions. As demonstrated in [3] these advantages are brought by the use of explicit models conjugating spatial and temporal priors. Reference [3] also shows that LQG should bring even larger gains for ELTs. LQG is also shown to exhibit a good robustness to wind speed profile uncertainties, which is important for on-sky operation.

LQG control is now available and tested on the DARC RTC platform [2], laboratory tests have begun at Meudon observatory and on-sky tests are planned in summer 2012 at the *William Herschel Telescope*.

Acknowledgements

We thank the Agence Nationale de la Recherche for supporting this work under the project CHAPER-SOA ANR-09-BLAN-0162-01. We also thank the European Commission under FP7 Grant Agreement No. 266404 Optical Infrared Coordination Network for Astronomy. We finally thank G. Rousset and colleagues (Paris Observatory), T.-J. Morris, A.-G. Basden and colleagues (University of Durham), P. Massioni (University Paris 13 and Onera), C. Petit and S. Meimon (Onera) for fruitful discussions.

References

1. A. Basden, D. Geng, R. Myers, and E. Younger. Durham adaptive optics real-time controller. *Applied Optics*, 49:6354–6363, November 2010.
2. A. Basden, R. Myers, N. Dipper, E. Younger, T. Morris, D. Geng, and S. Dimoudi. Are integral controllers adapted to the new era of ELT adaptive optics? In *Adaptative Optics for Extremely Large Telescopes 2*, 2012.
3. J.-M. Conan, H.-F. Raynaud, C. Kulcsár, S. Meimon, and G. Sivo. Are integral controllers adapted to the new era of ELT adaptive optics? In *Adaptative Optics for Extremely Large Telescopes 2*, 2012.
4. C. Correia, J.-M. Conan, C. Kulcsár, H.-F. Raynaud, and C. Petit. Adapting optimal LQG methods to ELT-sized AO systems. In *Adaptative Optics for Extremely Large Telescopes*, 2010.
5. J.-G. Cuby, S. Morris, T. Fusco, M. Lehnert, P. Parr-Burman, G. Rousset, J.-P. Amans, S. Beard, I. Bryson, M. Cohen, N. Dipper, C. Evans, M. Ferrari, E. Gendron, J.-L. Gimenez, D. Gratadour, P. Hastings, Z. Hubert, E. Hugot, P. Jagourel, P. Laporte, V. Lebrun, D. Le Mignant, F. Madec, R. Myers, B. Neichel, T. Morris, C. Robert, H. Schnetler, M. Swinbank, G. Talbot, W. Taylor, F. Vidal, S. Vivès, P. Vola, N. Welikala, and M. Wells. EAGLE: a MOAO fed multi-IFU NIR

workhorse for E-ELT. In *SPIE Conference*, volume 7735 of *Society of Photo-Optical Instrumentation Engineers (SPIE) Conference Series*, July 2010.

6. E. Gendron, F. Vidal, M. Brangier, T. Morris, Z. Hubert, A. Basden, G. Rousset, R. Myers, F. Chemla, A. Longmore, T. Butterley, N. Dipper, C. Dunlop, D. Geng, D. Gratadour, D. Henry, P. Laporte, N. Looker, D. Perret, A. Sevin, G. Talbot, and E. Younger. MOAO first on-sky demonstration with CANARY. *A&A*, 529:L2, May 2011.
7. F. Hammer, F. Sayède, E. Gendron, T. Fusco, D. Burgarella, V. Cayatte, J.-M. Conan, F. Courbin, H. Flores, I. Guinouard, L. Jocou, A. Lançon, G. Monnet, M. Mouhcine, F. Rigaud, D. Rouan, G. Rousset, V. Buat, and F. Zamkotsian. The FALCON Concept: Multi-Object Spectroscopy Combined with MCAO in Near-IR. In J. Bergeron & G. Monnet, editor, *Scientific Drivers for ESO Future VLT/VLTI Instrumentation*, page 139, 2002.
8. E. Marchetti, R. Brast, B. Delabre, R. Donaldson, E. Fedrigo, C. Frank, N. Hubin, J. Kolb, J.-L. Lizon, M. Marchesi, S. Oberti, R. Reiss, C. Soenke, S. Tordo, A. Baruffolo, P. Bagnara, A. Amorim, and J. Lima. MAD on sky results in star oriented mode. In *SPIE Conference*, volume 7015 of *Society of Photo-Optical Instrumentation Engineers (SPIE) Conference Series*, July 2008.
9. P. Massioni, C. Kulcsár, H.-F. Raynaud, and J.-M. Conan. Fast computation of an optimal controller for large-scale adaptive optics. *Journal of the Optical Society of America A*, 28:2298, November 2011.
10. S. Meimon, C. Petit, T. Fusco, and C. Kulcsár. Tip-tilt disturbance model identification for Kalman-based control scheme: application to XAO and ELT systems. *Journal of the Optical Society of America A*, 27(26):A260000, September 2010.
11. N. M. Milton, M. Lloyd-Hart, C. Baranec, T. Stalcup, Jr., K. Powell, D. McCarthy, C. Kulesa, and K. Hege. Commissioning the MMT ground-layer and laser tomography adaptive optics systems. In *SPIE Conference*, volume 7015 of *Society of Photo-Optical Instrumentation Engineers (SPIE) Conference Series*, July 2008.
12. R. M. Myers, Z. Hubert, T. J. Morris, E. Gendron, N. A. Dipper, A. Kellerer, S. J. Goodsell, G. Rousset, E. Younger, M. Marteaud, A. G. Basden, F. Chemla, C. D. Guzman, T. Fusco, D. Geng, B. Le Roux, M. A. Harrison, A. J. Longmore, L. K. Young, F. Vidal, and A. H. Greenaway. CANARY: the on-sky NGS/LGS MOAO demonstrator for EAGLE. In *SPIE Conference*, volume 7015 of *Society of Photo-Optical Instrumentation Engineers (SPIE) Conference Series*, July 2008.
13. R. Penrose. A generalized inverse for matrices. *Proceedings of the Cambridge Philosophical Society*, 51:406–413, July 1955.
14. C. Petit, J.-M. Conan, C. Kulcsár, and H.-F. Raynaud. Linear quadratic Gaussian control for adaptive optics and multiconjugate adaptive optics: experimental and numerical analysis. *Journal of the Optical Society of America A*, 26:1307, May 2009.
15. F. Roddier. Book Review: Adaptive optics in astronomy / Cambridge U Press, 1999. *Irish Astronomical Journal*, 26:171, 1999.
16. F. Vidal, E. Gendron, and G. Rousset. Tomography approach for multi-object adaptive optics. *Journal of the Optical Society of America A*, 27(26):A260000, October 2010.
17. F. Zernike. Diffraction theory of the knife-edge test and its improved form, the phase-contrast method. *MNRAS*, 94:377–384, March 1934.